A Numerical Solution Technique for Multitemperature Plasma Hydrodynamics

C. R. DeVore and J. H. Gardner

Laboratory for Computational Physics

April 11, 1985

DTIC
ELECTE
APR 23 1985
D

NAVAL RESEARCH LABORATORY
Washington, D.C.

AD-A152 701

DTIC FILE COPY

REPORT DOCUMENTATION PAGE

1a REPORT SECURITY CLASSIFICATION UNCLASSIFIED		1b RESTRICTIVE MARKINGS		
2a SECURITY CLASSIFICATION AUTHORITY		3 DISTRIBUTION/AVAILABILITY OF REPORT Approved for public release; distribution unlimited.		
2b DECLASSIFICATION/DOWNGRADING SCHEDULE				
4 PERFORMING ORGANIZATION REPORT NUMBER(S) NRL Memorandum Report 5540		5 MONITORING ORGANIZATION REPORT NUMBER(S)		
6a NAME OF PERFORMING ORGANIZATION Naval Research Laboratory	6b OFFICE SYMBOL (If applicable) Code 4040	7a NAME OF MONITORING ORGANIZATION		
6c ADDRESS (City, State, and ZIP Code) Washington, DC 20375-5000		7b. ADDRESS (City, State, and ZIP Code)		
8a NAME OF FUNDING/SPONSORING ORGANIZATION	8b OFFICE SYMBOL (If applicable)	9 PROCUREMENT INSTRUMENT IDENTIFICATION NUMBER		

8c ADDRESS (City, State, and ZIP Code)	10 SOURCE OF FUNDING NUMBERS			
	PROGRAM ELEMENT NO	PROJECT NO IA- DEAI08- 79DP40092	TASK NO	WORK UNIT ACCESSION NO DN220-133

11 TITLE (Include Security Classification)

A Numerical Solution Technique for Multitemperature Plasma Hydrodynamics

12 PERSONAL AUTHOR(S)
DeVore, C.R. and Gardner, J.H.

13a TYPE OF REPORT Interim	13b. TIME COVERED FROM _____ TO _____	14 DATE OF REPORT (Year, Month, Day) 1985 April 11	15. PAGE COUNT 27

16 SUPPLEMENTARY NOTATION

This research was supported by the Office of Naval Research and the Department of Energy.

17	COSATI CODES		18 SUBJECT TERMS (Continue on reverse if necessary and identify by block number)
FIELD	GROUP	SUB-GROUP	Numerical finite difference Multitemperature plasma hydro-
			Two-temperature plasma dynamics

19 ABSTRACT (Continue on reverse if necessary and identify by block number)

We describe a numerical technique for the solution of the equations of multitemperature plasma hydro-dynamics in a finite-difference formulation. A key feature of the algorithm is that it is locally mass, momentum, and energy conservative, and therefore is particularly useful for problems which require an accurate description of each of the constitutent fluids in the presence of shock waves. We present explicit formulae for solving the equations for a simple two-temperature plasma, and discuss the extension of the algorithm to more complex multitemperature plasma models. We also summarize some results from a two-temperature laser-matter interaction simulation as an illustration of the performance of the algorithm.

20 DISTRIBUTION AVAILABILITY OF ABSTRACT ☒ UNCLASSIFIED/UNLIMITED ☐ SAME AS RPT ☐ DTIC USERS	21 ABSTRACT SECURITY CLASSIFICATION UNCLASSIFIED	
22a NAME OF RESPONSIBLE INDIVIDUAL C. R. DeVore	22b TELEPHONE (Include Area Code) (202) 767-3196	22c OFFICE SYMBOL Code 4040

DD FORM 1473, 84 MAR
83 APR edition may be used until exhausted
All other editions are obsolete

CONTENTS

iii

A NUMERICAL SOLUTION TECHNIQUE FOR MULTITEMPERATURE PLASMA HYDRODYNAMICS

INTRODUCTION

There are many problems in computational plasma dynamics in which a multitemperature fluid treatment of the plasma is sufficiently complex to adequately describe the phenomena of primary interest, yet is sufficiently simple to permit a thorough study of the phenomena without a prohibitive expenditure of resources. In a multitemperature approach the various particle species, and perhaps the radiation field, are modeled as distinct, interacting fluids which exchange energy at a finite rate through collisional or collisionless processes, while the exchange of momentum is assumed to be sufficiently rapid that the velocities of the component fluids are identical. The frequent application of these models to laboratory and astrophysical time-dependent plasma phenomena make valuable a computational approach to solving the equations which is accurate, efficient, and of general utility.

We describe a numerical method for solving the multitemperature plasma hydrodynamics equations in a timestep-split, finite-difference formulation. Our algorithm possesses several important characteristics. We solve the convective transport equations for the mass, momentum, and total energy densities in conservation form, thereby guaranteeing that the plasma mass, momentum, and total energy be locally (and therefore globally) conserved. At the same time, we also solve the convective transport equations for the internal energy densities of each of the individual species, renormalizing the resulting solutions so that they are consistent with the total energy equation. In this way, we simultaneously achieve local conservation of total energy and comparable accuracy in the description of each of the plasma

1

species. This solution of an overdetermined set of hydrodynamic equations is a unique feature of the algorithm. Our method of solution yields a superior description of shock wave propagation in the plasma, also as a consequence of integrating the equations in conservation form. We treat the temperature equilibration between species in a fully implicit manner in the diffusive transport step, and as a result equilibration timescales much shorter than the hydrodynamic timescales in the problem can be accomodated. A second novel feature of the algorithm is the inclusion of the temperature changes induced by the convection as source terms in the diffusive transport calculation. The hydrodynamic heating then acts simultaneously with the other processes – temperature equilibration, thermal conduction, etc. – which determine the species' temperatures. Finally, for problems in which an implicit calculation of the thermal conduction terms for more than one of the plasma species is necessary, we solve the coupled temperature equations using an efficient iterative scheme.

The simplest example of a multitemperature plasma is a two-temperature model of a plasma composed solely of electrons and ions. This model contains all of the essential elements of the general approach, and we therefore describe in detail the solution procedure for this simple case. We conclude with some remarks about the use of the algorithm and its generalization to more complex plasma models.

THE BASIC EQUATIONS OF THE TWO-TEMPERATURE MODEL

We begin by considering the simple case of a two-component plasma of electrons and ions. We further assume that the plasma is charge-neutral and that the exchange of momentum between the electron and ion fluids is perfect, so that the plasma is also current-free. The numerical algorithm that we use to solve this problem readily generalizes to situations involving a larger number of interacting fluids. The four basic equations of the model [1,2] are the transport equations for the mass density ρ, the momentum density $\rho\vec{v}$, the electron internal energy density U_e, and the ion internal energy density U_i,

$$\frac{\partial \rho}{\partial t} + \nabla \cdot (\rho\vec{v}) = 0, \tag{1}$$

$$\frac{\partial}{\partial t}(\rho\vec{v}) + \nabla \cdot (\rho\vec{v}\vec{v}) + \nabla P = 0, \tag{2}$$

$$\frac{\partial U_e}{\partial t} + \nabla \cdot (U_e \vec{v}) + P_e(\nabla \cdot \vec{v}) = S_e, \tag{3}$$

and

$$\frac{\partial U_i}{\partial t} + \nabla \cdot (U_i \vec{v}) + P_i(\nabla \cdot \vec{v}) = S_i. \tag{4}$$

The other quantities in these equations are the partial pressures P_e and P_i and the energy source terms S_e and S_i. We can combine Eqs. (1)-(4) to obtain a fifth equation, for the total energy density $E = \frac{1}{2}\rho v^2 + U_e + U_i$:

$$\frac{\partial E}{\partial t} + \nabla \cdot ([E+P]\vec{v}) = S, \tag{5}$$

3

where $P = P_e + P_i$ is the total pressure and $S = S_e + S_i$ is the source term for the total energy. Specification of equations of state for the two species completes the set of fundamental relations of the model.

The energy source terms in Eqs. (3)–(5) describe the local deposition and dissipation of energy due to any processes relevant to the physical problem of interest, e.g., temperature equilibration between species, the conduction of heat through the plasma, bremmstrahlung radiation losses, etc. The thermal coupling of the two fluids leads to an energy exchange rate X, so we rewrite the electron and ion source terms S_e and S_i as

$$S_e = Q_e - X \tag{6}$$

and

$$S_i = Q_i + X. \tag{7}$$

We adopt for the exchange rate X its form for an ideal plasma [1,2],

$$X = C_v \omega (T_e - T_i), \tag{8}$$

in which C_v is the specific heat capacity at constant volume for an ideal electron gas, ω is the reciprocal of the temperature equilibration time, and T_e and T_i are the electron and ion temperatures.

4

THE SOLUTION TECHNIQUE FOR THE TWO-TEMPERATURE MODEL

We now proceed to solve the initial-boundary value problem posed by Eqs. (1)-(4), together with Eqs. (6)-(8) for the energy source terms. Our method of solution is based on an Eulerian, finite-difference discretization of the equations, in which we timestep-split the convective transport from the dissipative processes. The splitting permits us to employ an explicit numerical scheme to solve the convective transport problem and an implicit scheme to solve the diffusive transport problem. Significant computational savings can result from this approach if the dissipative processes, specifically in this case the temperature equilibration, have characteristic timescales shorter than the hydrodynamic timescale determined by the Courant-Friedrichs-Lewy stability condition [3]. If the convective and diffusive timescales are greatly disparate, however, the solutions which are obtained should be tested for their sensitivity to the numerical timestep employed.

In the convective transport step, we solve the overdetermined set of hydrodynamic equations, Eqs. (1)-(5), setting $S_e = S_i = S = 0$. We use a flux-corrected transport [4] algorithm to integrate the equations. The positivity property of flux-corrected transport gives it an advantage over alternative conservative numerical schemes, e.g. Lax-Wendroff [5] or conservative leapfrog [6], which may in principle also be used. Given values for all of the physical variables at time t (step n), we begin by integrating these equations forward to time $t + \Delta t$ (step n+1), symbolically

$$\{\rho^n, (\rho\vec{v})^n, E^n, U_e^n, U_i^n\} \rightarrow$$

$$\{\rho^{n+1}, (\overrightarrow{\rho v})^{n+1}, E^{\prime n+1}, U_e^{\prime\prime n+1}, U_i^{\prime\prime n+1}\}.$$

We may now calculate the total internal energy density U either as the sum of the partial internal energy densities U_e and U_i, or as the difference between the total energy density and the kinetic energy density,

$$U^{\prime n+1} = E^{\prime n+1} - \frac{[(\overrightarrow{\rho v})^{n+1}]^2}{2\rho^{n+1}}. \qquad (9)$$

These two results are of course not numerically identical, owing to the truncation errors in the differencing of the convective and source terms in the equations. We adopt Eq. (9) as the correct expression for the total internal energy density, thereby ensuring that energy is conserved locally in the convective transport calculation. As a consequence, we must specify a prescription for correcting the partial internal energy densities so that their sum is equal to the total given by Eq. (9).

We distribute the numerical error in the calculation of the total internal energy density locally among the partial internal energy densities in the following way. Assigning fractional errors ε_e and ε_i to the electrons and ions, we calculate at each mesh point

$$U_s^{\prime n+1} = U_s^{\prime\prime n+1} + \varepsilon_s [U^{\prime n+1} - (U_e^{\prime\prime n+1} + U_i^{\prime\prime n+1})], \qquad s = e, i. \qquad (10)$$

Requiring that $\varepsilon_e + \varepsilon_i = 1$, we have

6

$$U_e^{'n+1} + U_i^{'n+1} = U^{'n+1}, \tag{11}$$

as desired. A prescription for distributing the error, i.e., an expression for ϵ_s, is to be selected. Our choice is to take ϵ_s proportional to $U_s^{''n+1}$; this amounts to assuming the same percentage error for each of the partial internal energy densities, and leads to the renormalization formulae

$$U_s^{'n+1} = \frac{U_s^{''n+1}}{U_e^{''n+1} + U_i^{''n+1}} U^{'n+1}, \qquad s = e, i. \tag{12}$$

Alternative prescriptions for distributing the error are certainly available, e.g., assuming a fixed percentage error for the internal energy per particle and setting ϵ_s proportional to the local number density n_s. We prefer the prescription above because of the simplicity of Eqs. (12) for the corrected partial internal energy densities.

By solving the conservation equations for the mass, momentum, and total energy densities, we guarantee local conservation of mass, momentum, and energy in the calculation, and we ensure that the Rankine-Hugoniot conditions are satisfied across any shocks that develop in the plasma. At the same time, we calculate the internal energy densities for the various species independently of one another, so that the state of each of the plasma constituents is known with roughly the same accuracy. There are two obvious alternatives to this approach.

The first alternative is to solve the total energy equation and the

7

internal energy equation for one of the species, then compute the internal energy of the other species by subtraction. This is equivalent to setting the fractional error ε_s to unity for the second species. The internal energy density obtained in this manner, and therefore the pressure and temperature derived from it, is prone to large errors when the various energies in the problem differ by orders of magnitude. Our algorithm is certainly not immune to such difficulties, since we calculate the total internal energy density by subtraction (Eq. (9)). Fortunately, this problem is self-correcting as the calculation progresses, owing to the compressional and conduction heating induced by the abnormally low pressures and temperatures in the regions where the internal energy becomes negative. Our method of solution at least has the advantage of describing each of the species with comparable accuracy throughout the plasma.

The second alternative is to solve only the equations for the partial internal energies. This approach in general requires specification of an artificial viscosity term [7] and the inclusion of viscous stresses in the momentum equation and viscous heating in the internal energy equation for at least one of the plasma species. By judicious choice of the viscosity coefficients, global conservation of energy can be achieved. Our approach has the advantage of not requiring the introduction of an artificial viscosity, and yet guarantees local energy conservation in a straightforward manner. Furthermore, it is quite generally more satisfactory for problems in which shock waves are present. Numerical studies [8,9] show that the shock speed and profile are consistently more accurately determined in an energy conservative formulation than in a nonconservative formulation.

8

We now turn to the diffusive transport calculation. In the diffusive transport step the plasma is held stationary ($\vec{v} = 0$) and the mass density remains at its value at the end of the convective transport step. As the intermediate values for the diffusive transport calculation we take the mass density ρ^{n+1} at the end of the current convective transport step and the temperatures T_e^n and T_i^n from the preceding diffusive transport step. We formally treat the temperature changes induced by the convection – the hydrodynamic heating rates – as additional source terms in the energy equations, subject to redistribution among the species by the thermal coupling between the fluids. We adopt this procedure in order to avoid potential convergence difficulties, arising in regions where the temperature equilibration is very fast, caused by allowing the convection to drive the temperatures apart in the convective step and then having the temperature equilibration attempt to force them back together in the subsequent diffusive step.

With the inclusion of the rates of hydrodynamic heating H_e and H_i, the equations for the diffusive transport calculation, obtained from Eqs. (3) and (4), are

$$C_{ve} \frac{\partial T_e}{\partial t} = Q_e - C_v \omega (T_e - T_i) + H_e \tag{13}$$

and

$$C_{vi} \frac{\partial T_i}{\partial t} = Q_i + C_v \omega (T_e - T_i) + H_i, \tag{14}$$

9

10. Christiansen, J. P., and K. V. Roberts, J. Comput. Phys. 17 (1975) 332.

11. Laasonen, P., Acta Math. 81 (1949), 309.

12. Crank, J., and P. Nicholson, Proc. Cambridge Philos. Soc. 43 (1947) 50.

13. Gardner, J. H., and S. E. Bodner, Phys. Rev. Lett. 47 (1981) 1137.

REFERENCES

1. Spitzer, L., Jr., "Physics of Fully Ionized Gases", 2nd ed.,
   Interscience, New York, 1961.

2. Braginskii, S. I., Transport Processes in a Plasma, in Reviews of Plasma
   Physics" (M. A. Leontovich, ed.), Vol. 1, p. 205, Consultants Bureau,
   New York, 1965.

3. Courant, R., K. O. Friedrichs, and H. Lewy, Math. Ann. 100 (1928), 32.

4. Book, D. L., J. P. Boris, and S. T. Zaleszak, Flux-Corrected Transport,
   in "Finite-Difference Techniques for Vectorized Fluid Dynamics
   Calculations" (D. L. Book, ed.), Chap. 3, Springer-Verlag, New York,
   1981.

5. Lax, P. D., and B. Wendroff, Comm. Pure Appl. Math. 13 (1960), 217.

6. Potter, D., "Computational Physics", Chap. 3, Wiley-Interscience,
   Chichester, 1973.

7. von Neumann, J., and R. D. Richtmyer, J. Appl. Phys. 21 (1950), 232.

8. Gary, J., Math. Comput. 18 (1966) 1.

9. Colombant, D. G., and J. H. Gardner, J. Comput. Phys. 22 (1976) 389.
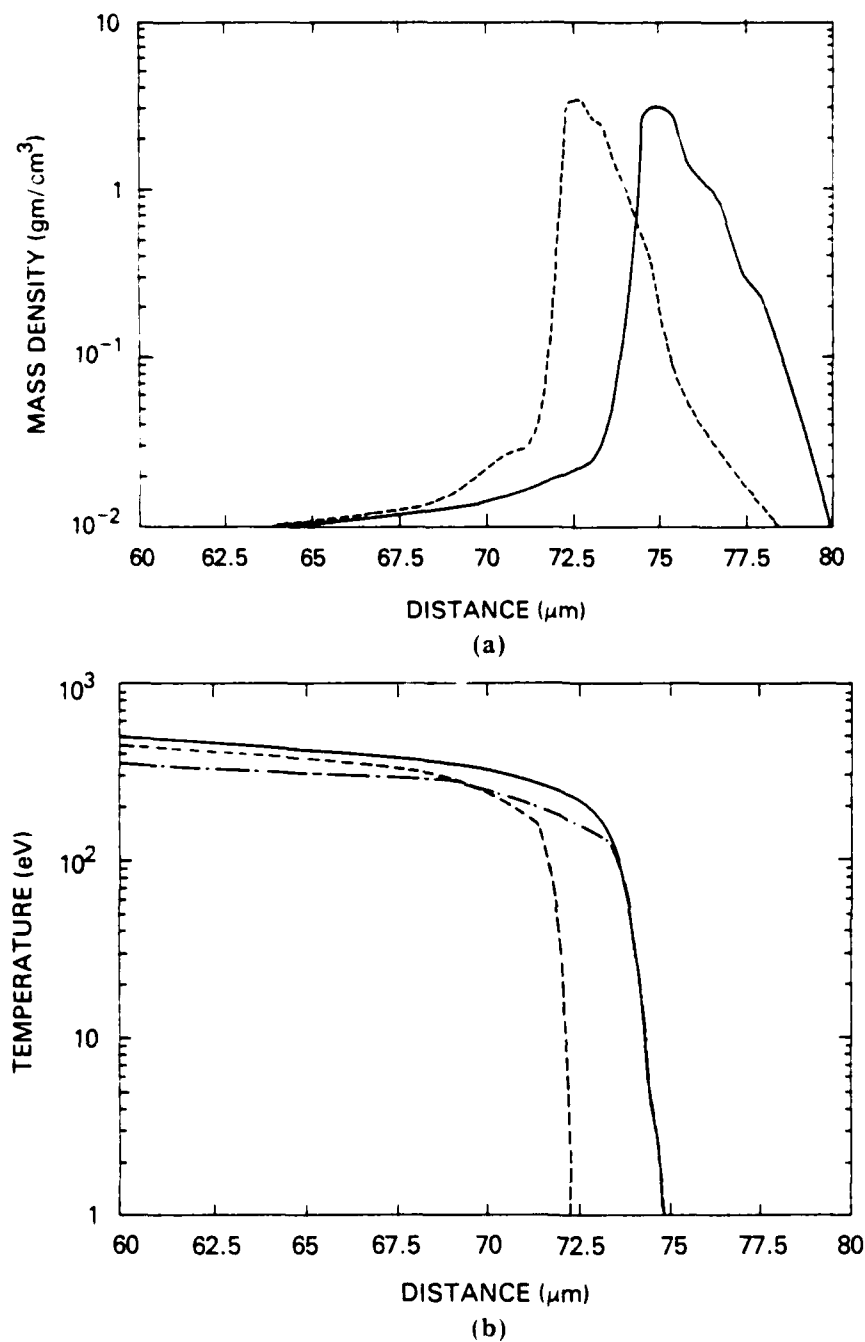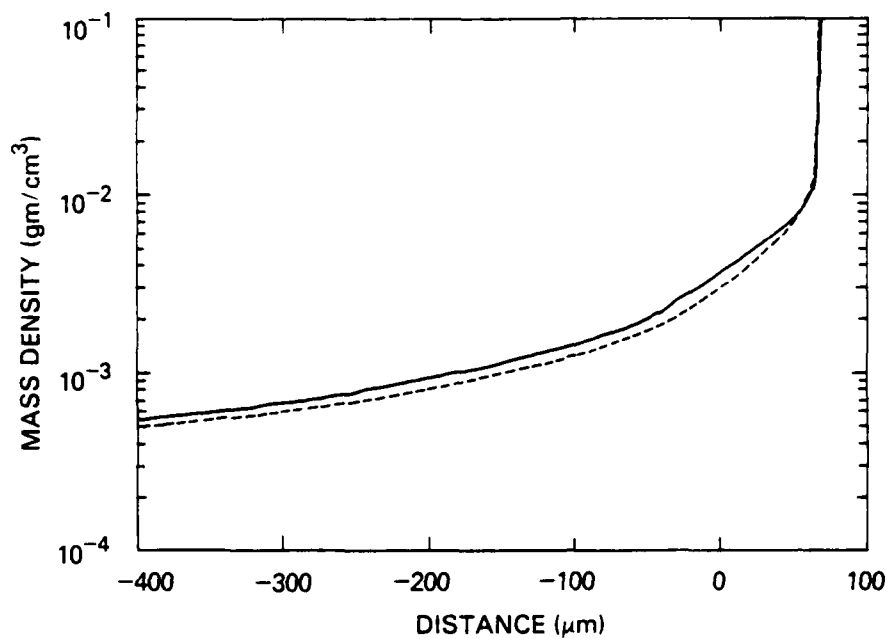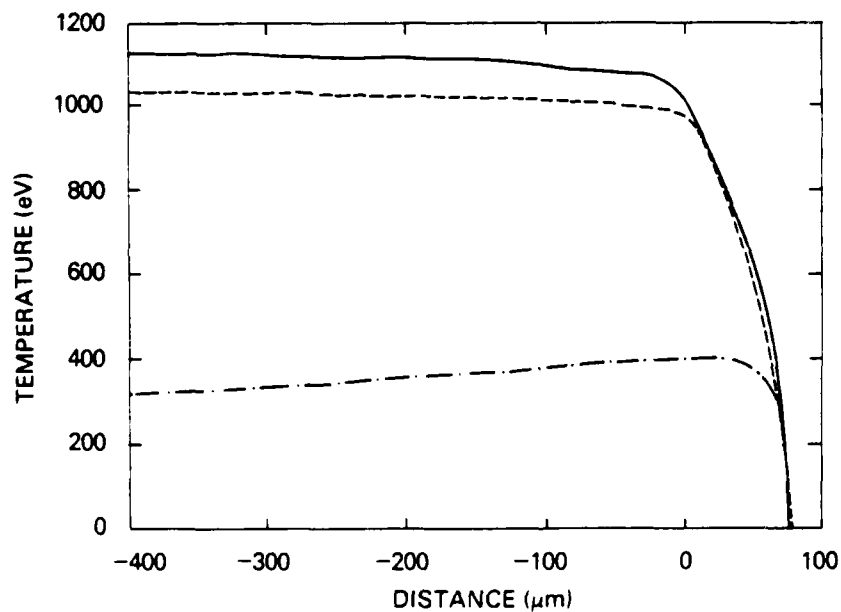
Figure 2. The mass densities and temperatures inside the critical surface at the peak of the laser pulse. The mass densities are shown in (a), for the two-temperature (——) and one-temperature (---) models. The temperatures are shown in (b), for the electrons (——) and the ions (-·-) in the two-temperature model and for the one-temperature model (---).

Figure 1. The mass densities and temperatures in the laser-irradiated target
at the peak of the laser pulse. The mass densities are shown in
(a), for the two-temperature (——) and one-temperature (---)
models. The temperatures are shown in (b), for the electrons
(——) and the ions (-·-) in the two-temperature model and for the
one-temperature model (---).

20

individual temperatures (corresponding to Eqs. (20) and (21)) are solved

iteratively in tandem with the 2(N-1) equations for the difference

temperatures and their source terms (corresponding to Eqs. (22) and (23)).

ACKNOWLEDGMENTS

DISCUSSION

The numerical algorithm that we use to solve the equations of the two-temperature plasma hydrodynamic model requires in the convective transport step the integration of the equation for the total energy, in addition to those for the mass, momentum, and partial internal energies. The cost is an increase of roughly 25% in the amount of numerical work done and in the computing time over methods which neglect either the total energy equation or one of the partial internal energy equations. The benefits are a guarantee of local conservation of total energy, a more accurate description of the propagation of shock waves through the plasma, and comparable accuracy in the computed fluid properties of each of the plasma species. In the diffusive transport step, the technique of iterating between equations for the species' temperatures and equations for the difference temperatures is useful for problems in which the conduction of heat by both species is sufficiently rapid to call for an implicit treatment. In simpler situations a direct solution of the coupled temperature equations is possible.

The extension of the algorithm to more general multitemperature plasma hydrodynamic models is straightforward. For an N-fluid model, the convective transport problem consists of the three equations for the mass, momentum, and total energy densities, and N equations for the partial internal energy densities. After calculating the total internal energy density from the solution of the first three equations, the separately computed partial internal energy densities are renormalized by an appropriate generalization of Eqs. (12). In the diffusive transport step, the N equations for the

18

plot density and temperature profiles for the expanding, accelerating target at the peak of the pulse in Figures 1a,b. Profiles from a one-temperature model calculation are shown for comparison with the two-temperature results. The temperature equilibration time varies from about 50 ns in the blowoff plasma to less than 1 ps in the core. The ion temperature peaks at 400 ev near the critical surface, where thermal coupling between the electrons and ions is still effective, and then declines outward from that point as the ion fluid cools by expansion. The electron temperature exhibits a monotonic increase to 1100 ev at the edge of the foil, due to inverse bremmstrahlung absorption in the underdense plasma. We plot the density and temperature profiles inside the critical surface in Figures 2a,b. The electron and ion temperatures converge rapidly toward the core of the target, coalescing at about 100 ev and decreasing together to less than 1 ev within the ablation surface.

A LASER-MATTER INTERACTION SIMULATION

We have implemented the two-temperature algorithm in the one-dimensional numerical simulation code FAST1D [13]. This code was developed to study the plasma hydrodynamics of the interaction of intense laser radiation with material targets. The energy in the incident laser beam is absorbed primarily by the electrons in the target, which then equilibrate locally with the ions and convect and conduct energy out of the deposition region. Conditions in the irradiated material range from strong thermal coupling in the compressed, shock-heated core of the target to negligible coupling in the rapidly expanding blowoff plasma. In the simulations, we routinely achieve mass, momentum, and total energy conservation to within machine precision and agreement between the electron and ion temperatures in the strongly coupled portion of the target to better than one part in one thousand. On those occasions when the total internal energy in a computational zone is driven negative owing to numerical errors, the algorithm smoothly corrects the problem over several timesteps without difficulty. These simulations have tested the algorithm over an extreme range of physical conditions. Its robust performance suggests that it is a reliable method of solution for general hydrodynamic problems in multitemperature plasmas.

We simulated the response of a 6.5 μm polystyrene (CH) planar target to a gaussian laser pulse of wavelength 1.06 μm, peak intensity 2×10^{13} W/cm^2, and full-width half-maximum duration of 2.6 ns. The target is initially at rest at x = 0, at room temperature and solid density (1.03 gm/cm^3). The peak of the laser pulse is reached 5 ns after the start of the calculation. We

16

(26) and (27). This recalculation is necessary in order to maintain

consistency between the temperatures used in the diffusive transport step and

the internal energies used in the convective transport step. The integration

of the plasma hydrodynamic equations for the current timestep is now

complete.

the amount of computational work required, this conclusion being perhaps problem- and hardware-dependent.

We complete the diffusive transport calculation by updating the partial internal and total energy densities and the temperatures. Calculating the accumulated energy changes since the end of the convective transport step,

$$\Delta U_e = C_{ve}' (T_e^{n+1(\infty)} - T_e^n) - H_e \Delta t \tag{24}$$

and

$$\Delta U_i = C_{vi}' (T_i^{n+1(\infty)} - T_i^n) - H_i \Delta t, \tag{25}$$

where (∞) denotes the value at the end of the temperature iteration, we calculate

$$U_e^{n+1} = U_e'^{n+1} + \Delta U_e, \tag{26}$$

$$U_i^{n+1} = U_i'^{n+1} + \Delta U_i, \tag{27}$$

and

$$E^{n+1} = E'^{n+1} + \Delta U_e + \Delta U_i. \tag{28}$$

The final step is to recompute the temperatures T_e and T_i from the equations of state and the partial internal energy densities U_e and U_i given by Eqs.

14

We use these results to calculate χ from Eq. (23),

$$\{Q_e^{n+1(m)}, Q_i^{n+1(m)}\} \rightarrow \chi^{n+1(m)},$$

and then calculate τ from Eq. (22),

$$\chi^{n+1(m)} \rightarrow \tau^{n+1(m)}.$$

Finally, substituting the expressions for Q_e and Q_i into Eqs. (20) and (21), we solve them separately for T_e and T_i,

$$\tau^{n+1(m)} \rightarrow \{T_e^{n+1(m+1)}, T_i^{n+1(m+1)}\}.$$

The iteration cycle may now be carried out again, starting with the updated values for the temperatures T_e and T_i, and repeated until convergence is achieved.

As an alternative to the iterative method, we may solve the coupled implicit equations for the temperatures directly, using solution techniques for banded or sparse matrices. These direct methods require more computer memory and time to solve the equations than does the iterative method to cycle once, but the direct methods are of course one-pass operations. We have found in practice however that the iteration scheme converges very rapidly, typically to a tolerance of less than 1% in two or three cycles. Thus, the iterative method may have an advantage over the direct methods in

$$C_{ve}' \frac{T_e^{n+1} - T_e^n}{\Delta t} = Q_e^{n+1} + C_v' \omega' \tau^{n+1} + H_e, \tag{20}$$

$$C_{vi}' \frac{T_i^{n+1} - T_i^n}{\Delta t} = Q_i^{n+1} + C_v' \omega' \tau^{n+1} + H_i, \tag{21}$$

and

$$\tau^{n+1} = \frac{\tau^n + \chi^{n+1} \Delta t}{1 + \Omega' \Delta t}, \tag{22}$$

where

$$\chi^{n+1} = \frac{Q_e^{n+1} + H_e}{C_{ve}'} - \frac{Q_i^{n+1} + H_i}{C_{vi}'}. \tag{23}$$

We solve Eqs. (20)-(23) iteratively. We begin by taking the species' temperatures at the end of the previous diffusive transport step as the first iterate in the current step,

$$T_e^{n+1(1)} = T_e^n \quad \text{and} \quad T_i^{n+1(1)} = T_i^n,$$

where the numbers in parentheses are iteration indices. The iteration then proceeds generally as follows. From the expressions for the energy sources Q_e and Q_i, we calculate their values from T_e and T_i,

$$\{T_e^{n+1(m)}, T_i^{n+1(m)}\} \rightarrow \{Q_e^{n+1(m)}, Q_i^{n+1(m)}\}.$$

Dividing Eqs. (13) and (14) for the species temperatures by their respective heat capacities and subtracting them, we obtain

$$\frac{\partial \tau}{\partial t} = \chi - \Omega \tau, \tag{16}$$

where the difference temperature τ is defined by

$$\tau = T_e - T_i, \tag{17}$$

the source term χ is

$$\chi = \frac{Q_e + H_i}{C_{ve}} - \frac{Q_i + H_i}{C_{vi}}, \tag{18}$$

and the relaxation rate Ω is

$$\Omega = \frac{C_{ve} + C_{vi}}{C_{ve} C_{vi}} C_v \omega. \tag{19}$$

We difference Eqs. (13), (14), and (16) treating the difference temperature τ fully implicitly, and for the differencing of the thermal conduction terms in the energy sources Q_e and Q_i, we also choose a fully implicit treatment [11]. Christiansen and Roberts [10] describe a time-centered implicit treatment of the equilibration and diffusion [12] processes. Fixing the heat capacities and the inverse equilibration time at their values at the end of the convective transport step, we obtain

where C_{ve} and C_{vi} are the specific heat capacities at constant volume. The hydrodynamic heating rates are given in finite-difference form as

$$H_s = C_{vs}^{'n+1} \frac{T_s^{'n+1} - T_s^n}{\Delta t}, \qquad s = e, i, \tag{15}$$

in which we calculate the heat capacities and temperatures at step n+1 from the internal energy densities U_e' and U_i' at the end of the convective transport step. We calculate the intermediate values for the internal and total energy densities by subtracting the energy changes $H_e \Delta t$ and $H_i \Delta t$ associated with the compressional heating from U_e', U_i', and E' (see Eqs. (24)-(28) below).

We seek solutions of Eqs. (13) and (14) in which the temperature equilibration is treated implicitly. If the thermal conduction processes may be treated explicitly, then we trivially solve Eqs. (13) and (14) as two equations in two unknowns, at each mesh point. If an implicit treatment of the thermal conduction is required for only one species, we can eliminate the temperature of the other species algebraically and solve the resulting system of equations by standard techniques (e.g., tridiagonal matrix inversion for a three-point diffusion operator in one space dimension). We consider the more general case of an implicit calculation of the thermal conduction terms for both species, to which we apply an iterative solution technique. Our approach is an adaptation of the iterative method described by Christiansen and Roberts [10].

END

FILMED

5-85

DTIC